Origin of the Moving Groups and their Contribution to the Determination of the Large-scale Galactic Potential

T. Antoja, D. Fernández, F. Figueras, E. Moreno, B. Pichardo, J. Torra, O. Valenzuela

Abstract We evaluate the hypothesis that relates the formation of moving groups to the resonances of the non-axisymmetric component of the Galactic potential (spiral arms and central bar). We apply multiscale techniques to an extensive sample of more than 24000 stars of the solar neighbourhood to characterize the kinematic structures in the U–V–age–$[Fe/H]$ space. The observational data is compared with the distribution in the kinematic plane obtained through the computation of test particle orbits under analytic models for the potential. Results from two different models for the spiral structure and/or the Galactic bar are presented here. We show that the simulations near the position of the ILR -1:4 of the spiral structure and the OLR 1:2 of the Galactic bar are able to reproduce kinematic structures similar to the observed ones. We discuss the fundamental role of the age and metallicity distributions in the confirmation of the hypothesis.

1 Introduction

Although some moving groups (kinematic structures in the solar neighbourhood) were discovered more than 150 years ago, their origin is still unclear. Recently, it has been proposed that they have a dynamic or "resonant" origin. Rather than being composed by stars sharing a common origin and evolution, as Eggen originally proposed, some observational evidences seem to suggest that they may arise when a realistic Galactic potential is used (e.g. [6]). Specifically, some moving groups are

T. Antoja, D. Fernández, F. Figueras, J. Torra
Departament d'Astronomia i Meteorologia and IEEC-UB, Institut de Ciències del Cosmos de la Universitat de Barcelona, Martí i Franquès, 1, E-08028 Barcelona, Spain,
e-mail: tantoja@am.ub.es

E. Moreno, B. Pichardo, O. Valenzuela
Instituto de Astronomía, Universidad Nacional Autónoma de México, A.P. 70-264, 04510 México D.F., México, e-mail: barbara@astroscu.unam.mx

likely to be due to effects of resonances of the spiral structure and the Galactic bar [5, 15]. If this hypothesis is confirmed, these structures appear as a new and powerful tool for studying the Milky Way's large scale structure and dynamics. In this work, we want to contribute to this study in the observational and theoretical view. The comparison between observational data (Sect.3) and simulations (Sect. 4) using the same statistical techniques (briefly described in Sect.2) will eventually allow us to constrain the parameters and characteristics of the spiral arms and central bar of the Milky Way (discussion in Sect. 5).

2 The Statistical Method

We use the multiscale technique of the wavelet denoising (WD) to characterize the structures (i.e. establish their shape, size or statistical significance) in the U–V–age–$[Fe/H]$ space both for observational data and for simulations (MR software, [18, 2]). This method allows us to obtain a smooth distribution function from a discrete point distribution via a smoothing/filtering treatment at different scales that eliminates Poisson fluctuations. It consist of: i) wavelet transform (a trous algorithm), ii) multiresolution Wiener filtering at each scale which weights each coefficient according to its significance and iii) reconstruction of the wavelet-transformed and denoised data. It allows an automatic local filtering of the Poisson fluctuations and the analysis is not restricted to one specific scale or band-width because all scales are visualized at the same time in the final distribution [2].

3 The Observed Kinematic Structures

We present an extensive compilation of kinematic data for 24190 stars of the solar neighbourhood, together with ages for 16055 of them and metallicities for 13109 stars. The total sample is formed by the following catalogues: OBA stars [3, 19], FGK stars [12], M dwarfs [16, 4] and KM giants [8]. Errors and biases in these data are discussed in detail in [2].

We apply the WD to this sample to characterize the kinematic structures in the U–V–age–$[Fe/H]$ space. Fig. 1 (left) shows the density field in the U–V plane[1]. The WD technique definitely confirms that the dominant structures in the U–V plane are branches that connect some classic moving groups [17]: the Sirius, Coma Berenices, Hyades-Pleiades and Hercules branches. The first three branches are spaced at intervals of approximately 15 $\mathrm{km\,s^{-1}}$, with the Hercules branch located about 30 $\mathrm{km\,s^{-1}}$ from the Hyades-Pleiades branch. All branches present a negative slope of about 16° in the U–V plane. A clockwise rotation through this angle is applied to the

[1] U is the radial velocity component positive towards the Galactic Centre, V is the azimuthal velocity component positive towards the Galactic rotation and W the vertical component positive towards the north Galactic pole.

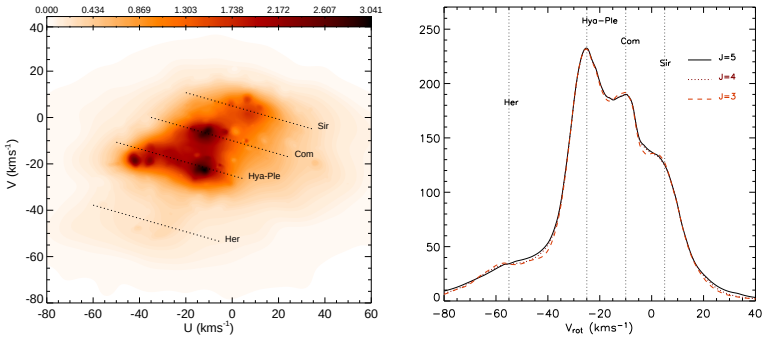

Fig. 1 Left: Density field in the U–V plane for the whole observational sample obtained by WD ($J_{plateau} = 4$, see [2]). **Right:** Density field for the direction perpendicular to the branches (V_{rot}).

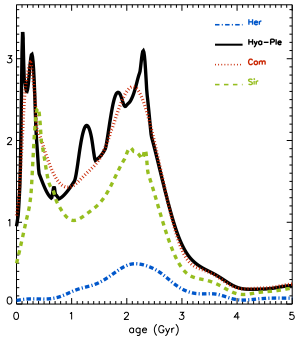

Fig. 2 Density of stars in each branch as a function of age worked out using the WD method for stars with $\varepsilon_{age} \leq 30\%$ (223, 1195, 1078 and 806 stars in the Hercules, Hyades-Pleiades, Coma Berenices and Sirius branches respectively).

original components (U, V) in order to align the new components (U_{rot}, V_{rot}) with the branches. Fig. 1 (right) shows the density distribution projected along V_{rot}. The four branches are clearly observed and their approximate positions are marked with vertical lines according to the maximums. We have studied ([2]) the density drops in this U–V plane and in the extremes of the branches: the existence of abrupt edge lines is confirmed, which definitely rules out the classic idea of a smooth velocity distribution.

We also study the age distribution of the stars of each branch (Fig. 2). An extended age distribution for all the branches is observed but each branch has a different minimum age: ~ 400 Myr for the whole set of the three branches of Hyades-Pleiades, Coma Berenices and Sirius, and 2 Gyr for the extended branch-like shape of Hercules. We also find certain clumps in the age distribution of the Hyades-Pleiades branch with a periodicity of about 500-600 Myr, maintained al least in the 0-2.5 Gyr range. For the other branches only a manifestation of the shape of the whole age distribution is observed.

4 The Simulations

The WD is applied to the distribution in the kinematic planes obtained through the numerical computation of test particle orbits. A random age τ in the range $[0, 2\,\mathrm{Gyr}]$ is assigned to each test particle. The integration is carried out from t$= -\tau$ to t$= 0$ (present time). The obtained phase space distributions at different galactic positions (boxes of 1 kpc) in the solar radius (8.5 kpc) and at $t = 0$ can be compared to the observed velocity distribution. From $3 \cdot 10^5$ to 10^6 test particles are born in a exponential disk with a scale length of 2.5 kpc within the galactocentric radii of 6 and 11 kpc and with an exponential vertical distribution with a scale length of 50 pc. The initial velocities are taken as a Gaussian distribution centred at the Regional Standard of Rest with $\sigma_U = \sigma_V = \sigma_W = 2\,\mathrm{km\,s^{-1}}$.

We employ a Galactic potential based on the one by [1] plus the non-axisymmetric components. The model for the Galactic bar [14] closely approximates Model S of [9] from COBE/DIRBE data: scale length of 4 kpc, axial ratios of 1.7:0.64:0.44 and angular velocity of 60 $\mathrm{km\,s^{-1}\,kpc^{-1}}$. We try two different masses: $9.8 \cdot 10^9$ and $1.4 \cdot 10^{10} M_\odot$. Two different models for the spiral structure are used:

- Model 1: the cosine perturbation by [11]
- Model 2: a 3D mass distribution obtained through the superposition of oblate spheroids along a given locus [13]

The parameters for the spiral structure are based mostly in observations (for details see [13]) and the locus is taken from [7]: 2 arms and a pitch angle of 15.5°. We vary its angular velocity Ω_p between 16 and 20 $\mathrm{km\,s^{-1}\,kpc^{-1}}$. The ratio of the radial component of the spiral arm field to the symmetrical field is 0.05 for Model 1 and the mass ratio between the arms and the disk is 0.05 for Model 2. The pattern speeds of the non-axysymmetric components locates the Sun near the 1:2 OLR of the bar and the -1:4 ILR of the spiral arms.

First we study the effects of Model 1 and 2 for the spiral structure on the velocity distribution near resonances. Fig. 3 shows the velocity distributions in a certain location of the solar radius for Model 1 with an angular velocity that locates the solar ring far from any resonance (left) and near the -1:4 ILR (middle). The model is not able to reproduce the observed structures in the U–V plane, except for the case with resonances influence where a structure similar to the Hyades-Pleiades moving group at $V < 0$ is formed. The effects of the -4:1 ILR for the model by [13] are lightly different (Fig. 3 right): these new model is able to reproduce by its own 4 groups or branches with positions and slope in the velocity plane similar to the real branches of Hyades-Pleiades, Sirius, Coma Berenices and Hercules[2].

The results of the joint effects of the spiral arms and the bar are shown in Fig.4 for different masses of the galactic bar. The main structures formed are coherent with the observational velocity distribution. We can see that the mass and the longitude of the bar are critical parameters. From these results we propose that such parameters can be constrained comparing these kinematic planes to the observed ones.

[2] Previous works have reported that this structure was consequence of the Galactic bar effects [5, 10].

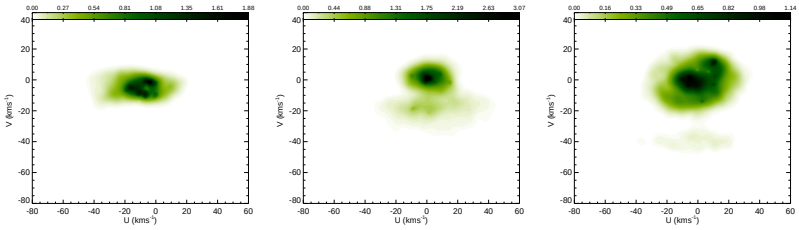

Fig. 3 Density field in the U–V plane in a given location of the solar radius for Model 1 (**left:** $\Omega_p = 16.7\,\mathrm{km\,s^{-1}\,kpc^{-1}}$, **middle:** $20\,\mathrm{km\,s^{-1}\,kpc^{-1}}$) and for Model 2 (**right:** $20\,\mathrm{km\,s^{-1}\,kpc^{-1}}$).

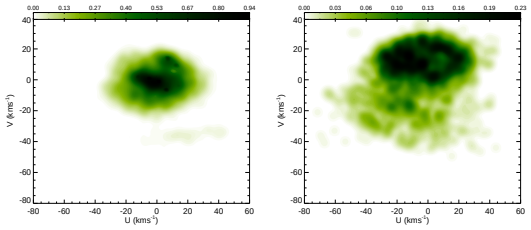

Fig. 4 Density field in the U–V plane in a given location of the solar radius with Model 2 ($\Omega_p = 20\,\mathrm{km\,s^{-1}\,kpc^{-1}}$) plus the Galactic bar (**left:** $M_{bar} = 9.8 \cdot 10^9 M\odot$, **right:** $M_{bar} = 1.4 \cdot 10^{10} M\odot$).

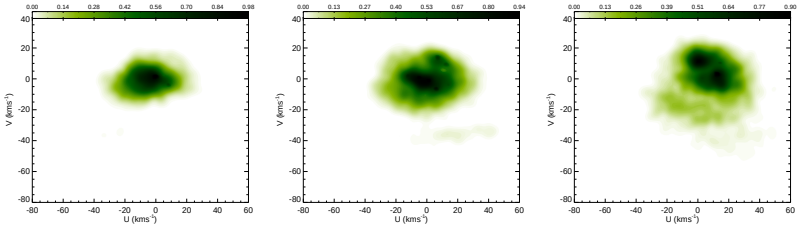

Fig. 5 Density field in the U–V plane at three different Galactic locations of the solar radius for Model 2 ($\Omega_p = 20\,\mathrm{km\,s^{-1}\,kpc^{-1}}$) plus the Galactic bar ($M_{bar} = 9.8 \cdot 10^9 M\odot$).

The kinematic planes in different Galactic positions using a unique model for the potential (Model 2 with $\Omega_p = 20\,\mathrm{km\,s^{-1}\,kpc^{-1}}$ plus the Galactic bar $M_{bar} = 9.8 \cdot 10^9 M\odot$) are shown in Fig.5. Again, we point out that the comparison between these kinematic planes and the observed one (see Fig. 1) can help to constrain the relative position of the Sun, spiral arms and bar. We state that the use of observational samples in different Galactic positions (RAVE, GAIA) will offer a more complete comparison.

5 Discussion

We have shown that the simulations of the kinematic plane, obtained by orbit integration of test particles, near the position of the ILR -1:4 of the spiral structure and the OLR 1:2 of the Galactic bar are able to reproduce kinematic structures similar to the observed ones. Furthermore, we have shown that our method can be used to constrain the parameters of the non-axisymmetric components of the potential. As an example, we state that significant differences in the simulated kinematic planes are observed when different models for the spiral arms are considered. [13] compared the potential and force fields produced by Model 1 and Model 2. They reported that the contributions to the potential from the entire pattern, which is not accounted for in Model 1, cause the local spiral potential to adopt shapes that are not correctly fit by the simple perturbing term that has been traditionally used. An exhaustive comparison between the two models is being undertaken.

Ages and metallicity distributions of the kinematic structures will play a fundamental role to confirm/refuse the hyphothesis that the kinematic branches in the solar neighbourhood have an origin related to the resonances of the spiral arms and the Galactic bar. The use of more and better ages and metallicity estimations as well as an improvement in the initial conditions of the simulations are required for the comparison e.g. of the kinematic-age planes.

Acknowledgements This research has been supported by MCyT under contracts ESP2006-26356-E, ESP2006-13855-C02-01 and AYA2006-15623-C02-02. T.A. was supported by the Predoctoral Fellowships of the Generalitat de Catalunya 2007FIC 00687 and 2008FIC 00121. We also thank support from LENAC mobility program.

References

1. Allen, C., Santillán, A. 1991, Rev. Mexicana Astron. Astrofis., 22, 255
2. Antoja, T., Figueras, F., Fernández, D., Torra, J. 2008, A&A, in press (arXiv:0809.0511)
3. Asiain, R., Figueras, F., Torra, J. et al. 1999, A&A, 341, 427
4. Bochanski, J.J., Hawley, S.L., Reid, I.N. et al. 2005, AJ, 130, 1871
5. Dehnen, W. 2000, ApJ, 119, 800
6. De Simone, R.S., Wu, X., Tremaine, S. 2004, MNRAS, 350, 627
7. Drimmel, R., Spergel, D.N. 2001, ApJ, 556, 181
8. Famaey, B., Jorissen, A., Luri, X., et al. 2005, A&A, 430, 165.
9. Freudenreich, H.T. 1998 ApJ, 492, 495
10. Fux, R. 2001, ApJ, 373, 511
11. Lin, C.C., Theory of the spiral structure. In *Highlights of Astronomy 4*, by Jager (Reidel Publ. Co., Dordrecht, Holland 1971), p.441
12. Nordström, B., Mayor, M., Andersen, J., et al. 2004, A&A, 418, 989
13. Pichardo, B., Martos, M., Moreno, E., et al. 2003, ApJ, 582, 230
14. Pichardo, B., Martos, M., Moreno, E. 2004, ApJ, 609, 144
15. Quillen, A.C., & Minchev, I. 2005, ApJ, 130,576
16. Reid, I.N., Gizis, J.E., Hawley, S.L. 2002, AJ, 124, 2721
17. Skuljan, J., Hearnshaw, J. B., Cottrell, P. L. 1999, MNRAS, 308, 731
18. Starck, J.L., & Murtagh, F. 2002, *Astronomical Image and data Analysis* (Springer)
19. Torra, J., Fernández, D., Figueras, F. 2000, A&A, 359, 82